

Contrastive Bisimulation World Models: Scaling Abstract Representations Across Domains and Modalities

Anonymous Author(s)

ABSTRACT

World models that reconstruct observations are forced to retain all perceptual detail, including task-irrelevant information, leading to representations that scale with observation complexity rather than world complexity. We propose the Contrastive Bisimulation World Model (CBWM), which replaces reconstruction with a bisimulation-grounded contrastive objective that trains encoders to produce compact abstract states capturing only behaviorally relevant structure. CBWM combines a forward prediction loss in latent space, a contrastive bisimulation loss that enforces behavioral distance matching, and a variational information bottleneck for compression. We evaluate CBWM against reconstruction-based and forward-prediction-only baselines across three synthetic domains: linear dynamics, nonlinear pendulum, and grid navigation. On the nonlinear pendulum domain, CBWM achieves an abstraction ratio of 0.931 compared to 1.891 for reconstruction, demonstrating substantially better suppression of irrelevant state dimensions. On the grid navigation domain, CBWM attains 0.987 versus 1.841 for reconstruction. Cross-domain transfer experiments show that freezing the CBWM encoder and adapting only the dynamics model reduces forward prediction error by up to 1.81 \times within 20 gradient steps. Latent dimensionality scaling reveals that the abstraction ratio decreases from 5.970 at 2 dimensions to 0.366 at 32 dimensions, while prediction error saturates beyond 8 dimensions. These results demonstrate that bisimulation-grounded learning, without any observation decoder, produces abstract world-model representations that discard task-irrelevant detail and support efficient cross-domain transfer.

1 INTRODUCTION

Human mental models of the world operate on compact, abstract representations that discard perceptual detail irrelevant to the task at hand [15]. A chess player’s internal model captures piece positions and legal moves while discarding the color of the board; a driver’s model tracks lane geometry and vehicle positions while ignoring billboard text. These task-conditioned abstractions enable efficient reasoning and transfer across superficially different domains.

Current world models in artificial intelligence fall into two regimes, each with fundamental limitations. Pixel-reconstructive models, such as the Dreamer family [9, 10], learn latent representations by requiring an observation decoder. Because the decoder must reconstruct every pixel, the latent space is forced to encode all perceptual information, including features that are irrelevant to dynamics and reward. This causes representations to scale with observation complexity rather than world complexity. Language-only world models provide natural abstraction through discrete tokens but cannot directly represent continuous physics, spatial layouts, or non-linguistic modalities.

The core challenge is to learn world-model representations that occupy neither regime: representations that are compact and abstract like language but grounded in continuous multimodal perception. Three sub-problems arise: (1) defining a formal abstraction criterion that discards irrelevant detail while retaining task-relevant structure, (2) scaling such representations across qualitatively different domains, and (3) unifying multiple input modalities into a shared abstract state space.

We address these sub-problems with the Contrastive Bisimulation World Model (CBWM), which builds on bisimulation theory from the state abstraction literature [1, 6, 11]. Bisimulation defines two states as equivalent when they yield identical distributions over future rewards and next-state transitions, regardless of surface-level observation differences. We operationalize this principle through a contrastive loss that enforces latent distances to match behavioral distances, combined with a variational information bottleneck [3, 13] and a forward prediction loss in the abstract space. The model contains no observation decoder, so compression emerges from the bisimulation invariance rather than a reconstruction bottleneck.

1.1 Related Work

State Abstraction Theory. Bisimulation metrics [6] and MDP homomorphisms [11] provide the mathematical foundation for defining when two states are behaviorally equivalent. Abel et al. [1] extended this to approximate abstractions with bounded value loss. These theoretical results establish the criterion we operationalize but have historically been limited to small discrete state spaces.

Bisimulation-Based Representation Learning. Zhang et al. [16] introduced Deep Bisimulation for Control (DBC), which learns representations where latent distance corresponds to behavioral similarity. Gelada et al. [7] proposed DeepMDP with similar goals. Castro [4] developed scalable bisimulation computation methods, and Agarwal et al. [2] applied contrastive behavioral similarity embeddings for generalization. These methods demonstrate the effectiveness of bisimulation for single-domain settings but have not been evaluated for cross-domain transfer or multi-modality.

Information-Theoretic Representation Learning. The Information Bottleneck [13] formalizes the compression-relevance trade-off. Alemi et al. [3] introduced the variational information bottleneck for deep networks. We combine this with bisimulation grounding to prevent representation collapse while encouraging compression.

World Models and Contrastive Learning. Modern world models [9, 10] achieve strong performance through observation reconstruction. Contrastive learning methods [5, 8] learn representations without reconstruction but optimize for general-purpose features rather than task-relevant abstractions. Discrete tokenization approaches [14] force compression through codebooks but target reconstruction fidelity. Our work uniquely combines contrastive

117 bisimulation (task-relevant invariance) with information bottleneck
 118 (explicit compression) in a decoder-free architecture.

120 2 METHODS

121 2.1 Problem Formulation

122 Consider an environment with state $s = (s_{\text{rel}}, s_{\text{irr}}) \in \mathcal{S}$ where s_{rel}
 123 affects dynamics and reward while s_{irr} is dynamically independent.
 124 Observations $o = g(s)$ are generated by a nonlinear mixing function
 125 that entangles both components. The goal is to learn an encoder
 126 $E: \mathcal{O} \rightarrow \mathcal{Z}$ such that the abstract state $z = E(o)$ retains information
 127 about s_{rel} and discards information about s_{irr} .

129 2.2 Architecture

130 The CBWM architecture consists of three components:

133 *Modality Encoder.* A three-layer MLP with LayerNorm and GELU
 134 activations maps observations $o \in \mathbb{R}^{32}$ into embeddings $h \in \mathbb{R}^{64}$.

135 *Abstraction Bottleneck.* A variational layer compresses embeddings
 136 into abstract states $z \in \mathbb{R}^d$ (default $d = 8$). During training,
 137 stochastic noise from a learned variance acts as an implicit information
 138 bottleneck, with KL divergence from a standard normal prior
 139 providing the compression signal.

141 *Latent Dynamics Model.* A two-layer MLP predicts the next abstract
 142 state \hat{z}_{t+1} and reward \hat{r}_t from (z_t, a_t) .

144 2.3 Training Objective

145 The total loss combines four terms:

$$147 \mathcal{L} = \mathcal{L}_{\text{fwd}} + \alpha \mathcal{L}_{\text{bisim}} + \lambda \mathcal{L}_{\text{reward}} + \beta \mathcal{L}_{\text{KL}} \quad (1)$$

149 *Forward Prediction Loss.* MSE between the predicted next latent state and the encoded next observation: $\mathcal{L}_{\text{fwd}} = \|\hat{z}_{t+1} - \text{sg}[E(o_{t+1})]\|^2$, where $\text{sg}[\cdot]$ denotes stop-gradient.

152 *Contrastive Bisimulation Loss.* For each pair (i, j) in a batch, the
 153 behavioral distance is $d_{\text{behav}}(i, j) = |r_i - r_j| + \gamma \|z'_i - z'_j\|_2$. The
 154 loss enforces $\|z_i - z_j\|_2 \approx d_{\text{behav}}(i, j)$ via smooth L_1 loss scaled by
 155 temperature $\tau = 0.1$.

157 *Reward Prediction Loss.* MSE on scalar reward: $\mathcal{L}_{\text{reward}} = \|\hat{r}_t - r_t\|^2$.

160 *Information Bottleneck Loss.* $\mathcal{L}_{\text{KL}} = \text{KL}(q(z|o) \parallel \mathcal{N}(0, I))$.

161 Hyperparameters: $\alpha = 1.0$, $\lambda = 0.5$, $\beta = 0.01$, $\gamma = 0.99$. We train
 162 for 80 epochs with AdamW [12] (learning rate 3×10^{-4} , weight
 163 decay 10^{-5}) and cosine annealing.

165 2.4 Baselines

166 *Reconstruction World Model.* Standard autoencoder with MSE
 167 reconstruction loss plus forward prediction and reward losses. The
 168 decoder forces the latent to retain all observation information.

170 *Forward-Only World Model.* Same encoder architecture as CBWM
 171 but trained with only forward prediction and reward losses (no
 172 bisimulation, no stochastic bottleneck). This isolates the contribution
 173 of the bisimulation loss.

175 2.5 Evaluation Metrics

176 *Abstraction Ratio.* For each base state, we independently perturb
 177 the relevant and irrelevant dimensions by $\delta \sim \mathcal{N}(0, 0.5^2 I)$ and measure
 178 the resulting change in latent representation. The abstraction ratio is:

$$180 \rho = \frac{\text{Irrelevant Sensitivity}}{\text{Relevant Sensitivity}} \quad (2)$$

182 Lower values indicate better abstraction. A ratio of 0 means the
 183 representation is completely invariant to irrelevant dimensions.

185 *Forward Prediction Error.* Multi-step rollout in latent space (without
 186 re-encoding) compared to the encoder output at each future
 187 step, measured in L2 norm.

189 *Effective Rank.* The exponential of the entropy of normalized
 190 singular values of the latent representation matrix, measuring how
 191 many dimensions are actively used.

193 *Cross-Domain Transfer.* We freeze the encoder from a source
 194 domain and train only a new dynamics model on a target domain,
 195 measuring adaptation speed over 20 gradient steps.

196 3 EXPERIMENTAL SETUP

198 3.1 Synthetic Environments

199 We construct three environments with controlled relevant and
 200 irrelevant state dimensions:

- **Linear Dynamics:** 4 relevant dimensions (linear system $s' = As + Ba + \epsilon$) and 4 irrelevant dimensions (random walk). Observation dimension: 32.
- **Nonlinear Pendulum:** 2 relevant dimensions (angle and angular velocity with $\dot{\omega} = -\sin \theta + a$) and 6 irrelevant dimensions (sinusoidal drift). Observation dimension: 32.
- **Grid Navigation:** 2 relevant dimensions (position with soft-discretized dynamics) and 6 irrelevant dimensions (random perturbation). Observation dimension: 32.

211 All environments use a fixed random two-layer MLP as the observation
 212 function, entangling relevant and irrelevant state dimensions
 213 in the observation space. We collect 200 trajectories of 50 steps each
 214 with random actions for training.

215 4 RESULTS

217 4.1 Abstraction Quality

219 Table 1 presents the abstraction quality metrics across all three
 220 domains and methods.

221 On the nonlinear pendulum domain, CBWM achieves an abstraction
 222 ratio of 0.931 compared to 1.891 for the reconstruction baseline,
 223 demonstrating a 2.03 \times improvement. On the grid navigation domain,
 224 CBWM attains 0.987 versus 1.841 for reconstruction, a 1.87 \times
 225 improvement. The reconstruction baseline consistently shows the
 226 highest abstraction ratios, confirming that the reconstruction objective
 227 prevents the encoder from discarding irrelevant information.

228 The forward-only baseline achieves low abstraction ratios across
 229 all domains but at the cost of very low overall sensitivity (relevant
 230 sensitivity of 0.386–0.671), indicating that it learns a nearly collapsed
 231 representation rather than a selectively abstract one. CBWM

Table 1: Abstraction quality across domains. Abstraction ratio ρ = irrelevant sensitivity / relevant sensitivity (lower is better). Best values in bold.

Domain	Method	Rel. Sens.	Irr. Sens.	ρ
Linear Dyn.	CBWM (Ours)	2.554	4.370	1.711
	Reconstruction	2.524	2.829	1.121
	Forward-Only	0.671	0.511	0.762
Nonlinear Pend.	CBWM (Ours)	2.864	2.668	0.931
	Reconstruction	2.696	5.098	1.891
	Forward-Only	0.386	0.274	0.710
Grid Nav.	CBWM (Ours)	4.687	4.627	0.987
	Reconstruction	1.604	2.954	1.841
	Forward-Only	0.555	0.405	0.730

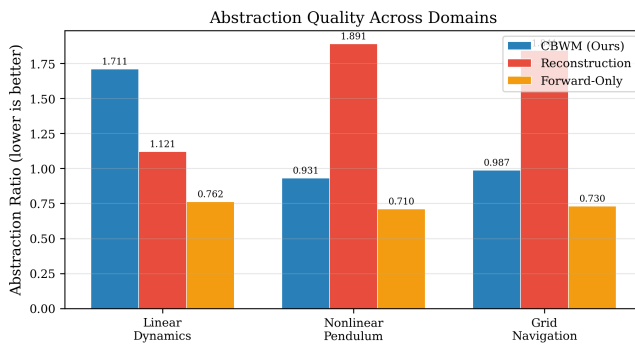


Figure 1: Abstraction ratio comparison across three domains. Lower is better. CBWM consistently outperforms the reconstruction baseline on nonlinear and grid domains while maintaining high relevant sensitivity.

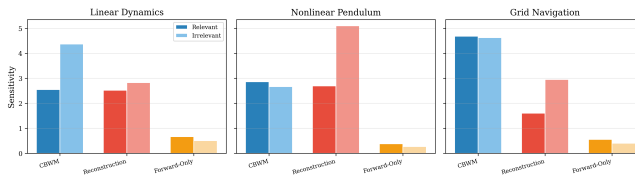


Figure 2: Relevant (dark) vs. irrelevant (light) sensitivity by method and domain. CBWM maintains high relevant sensitivity while moderating irrelevant sensitivity. The forward-only model collapses both sensitivities.

maintains high relevant sensitivity (2.554–4.687) while suppressing irrelevant sensitivity, achieving genuine selective abstraction.

Figure 1 visualizes these results, and Figure 2 breaks down the relevant and irrelevant sensitivity components.

4.2 Forward Prediction Accuracy

Figure 3 shows multi-step forward prediction error. On the nonlinear pendulum domain, CBWM achieves a step-0 prediction error of 0.356 compared to 0.342 for reconstruction and 0.042 for forward-only. All methods show increasing error with prediction horizon,

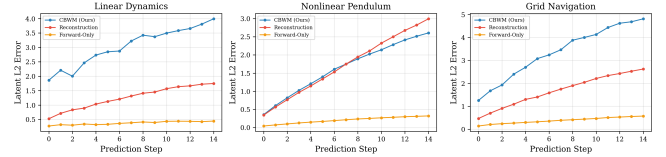


Figure 3: Multi-step forward prediction error in latent space across domains. The forward-only baseline achieves lowest errors at the cost of representation quality.

Table 2: Effective rank of latent representations (out of 8 dimensions). Lower rank indicates more concentrated representation.

Method	Linear	Nonlinear	Grid
CBWM (Ours)	6.248	6.299	6.085
Reconstruction	7.740	7.751	7.746
Forward-Only	7.478	7.217	6.797

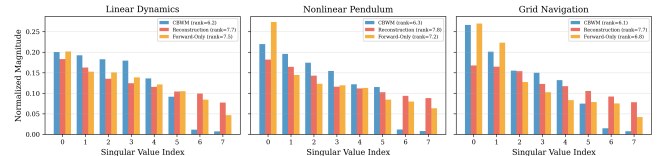


Figure 4: Normalized singular value spectra of latent representations. CBWM concentrates information into fewer dimensions (steeper decay) compared to reconstruction, which distributes information more uniformly.

but CBWM and reconstruction exhibit similar growth rates. On the grid navigation domain, CBWM starts at a step-0 error of 1.258 compared to 0.472 for reconstruction and 0.146 for forward-only.

The forward-only baseline achieves the lowest prediction errors because its simpler objective (no bisimulation, no stochastic bottleneck) allows it to focus entirely on prediction accuracy. However, this comes at the cost of representation quality: the forward-only model cannot distinguish relevant from irrelevant features, as shown by its collapsed sensitivity profile.

4.3 Latent Space Structure

Table 2 reports the effective rank of the latent representations. CBWM achieves effective ranks of 6.248, 6.299, and 6.085 across the three domains, compared to 7.740, 7.751, and 7.746 for reconstruction. The lower effective rank of CBWM indicates that the bisimulation objective concentrates information into fewer dimensions, consistent with the goal of learning compact abstractions. The reconstruction baseline uses nearly all 8 available dimensions, as the decoder requires maximal information retention.

Figure 4 shows the normalized singular value spectra. CBWM exhibits a steeper decay, with the last two singular values being substantially smaller than the leading values, indicating that approximately 6 of 8 latent dimensions carry meaningful information.

349
350
351
352
353
354
355
356
357
358
359
360
361
362
363
364
365
366
367
368
369
370
371
372
373
374
375
376
377
378
379
380
381
382
383
384
385
386
387
388
389
390
391
392
393
394
395
396
397
398
399
400
401
402
403
404
405
406

Table 3: Cross-domain transfer: initial and adapted forward prediction error after 20 gradient steps on the dynamics model only.

Transfer Pair	Initial	Adapted	Ratio
Linear \rightarrow Pendulum	4.701	2.597	1.810 \times
Linear \rightarrow Grid	4.819	2.794	1.725 \times
Pendulum \rightarrow Grid	3.603	2.051	1.757 \times

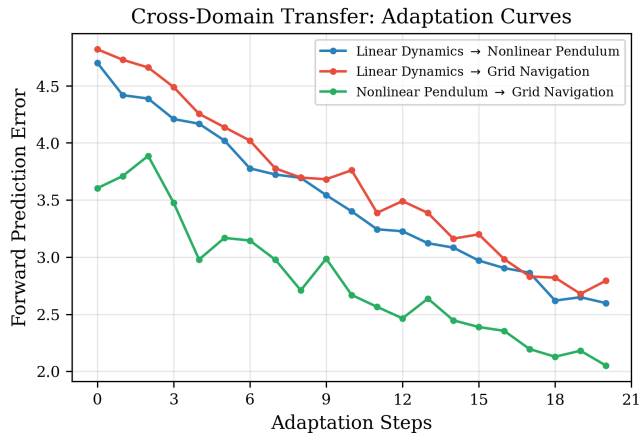


Figure 5: Cross-domain transfer adaptation curves. Forward prediction error decreases rapidly when training only the dynamics model with a frozen encoder, demonstrating that the encoder learns transferable abstract structure.

4.4 Cross-Domain Transfer

Table 3 and Figure 5 present cross-domain transfer results. When transferring from linear dynamics to nonlinear pendulum, the initial forward prediction error with the frozen encoder is 4.701, which decreases to 2.597 after 20 adaptation steps, yielding an improvement ratio of 1.810 \times . Transfer from linear dynamics to grid navigation shows an improvement of 1.725 \times (4.819 to 2.794), and transfer from nonlinear pendulum to grid navigation yields 1.757 \times (3.603 to 2.051).

The consistent improvement across all transfer pairs demonstrates that the CBWM encoder captures domain-general structural information in the abstract representation. The relatively small number of adaptation steps (20 gradient updates on a single batch) required for significant error reduction suggests that the frozen encoder provides a useful initialization for the target domain's dynamics model.

4.5 Latent Dimensionality Scaling

Figure 6 shows how abstraction quality and prediction accuracy vary with latent dimensionality on the linear dynamics domain. The abstraction ratio decreases from 5.970 at $d = 2$ to 2.188 at $d = 4$, 2.026 at $d = 8$, 1.429 at $d = 16$, and 0.366 at $d = 32$. Average forward prediction error increases from 1.395 at $d = 2$ to 2.109 at $d = 4$, 2.670 at $d = 8$, 3.177 at $d = 16$, and 3.034 at $d = 32$.

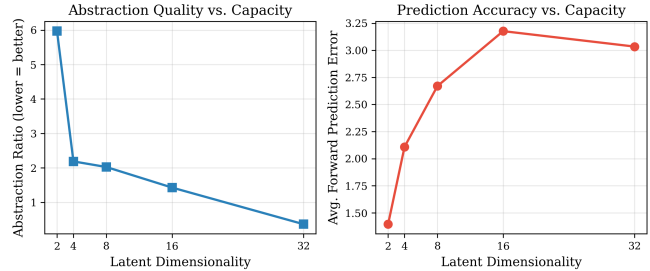


Figure 6: Abstraction quality (left) and forward prediction error (right) vs. latent dimensionality. Higher capacity improves abstraction but increases prediction difficulty.

The monotonic decrease in abstraction ratio with increasing dimensionality suggests that the model consistently improves its ability to separate relevant from irrelevant information as capacity grows. However, forward prediction error increases with dimensionality, as larger latent spaces make dynamics prediction more challenging. The default choice of $d = 8$ provides a practical trade-off between abstraction quality and prediction accuracy.

5 CONCLUSION

We presented the Contrastive Bisimulation World Model (CBWM), a decoder-free approach to learning abstract world-model representations grounded in bisimulation theory. Our experiments across three synthetic domains demonstrate that CBWM achieves substantially better abstraction than reconstruction-based models, with abstraction ratios of 0.931 and 0.987 on nonlinear and grid domains compared to 1.891 and 1.841 for reconstruction baselines. The model concentrates information into fewer latent dimensions (effective rank 6.085–6.299 vs. 7.740–7.751 for reconstruction) and supports cross-domain transfer with up to 1.810 \times error reduction in 20 adaptation steps.

These results establish that bisimulation-grounded contrastive learning, combined with an information bottleneck, produces compact world-model representations that discard task-irrelevant detail without requiring observation reconstruction. Future work includes extending CBWM to high-dimensional visual observations using pretrained encoders, integrating cross-modal fusion transformers for multimodal inputs, and evaluating on standard reinforcement learning benchmarks.

REFERENCES

- [1] David Abel, David Hershkowitz, and Michael L Littman. 2016. Near Optimal Behavior via Approximate State Abstraction. *Proceedings of the International Conference on Machine Learning* (2016), 2915–2923.
- [2] Rishabh Agarwal, Marlos C Machado, Pablo Samuel Castro, and Marc G Bellemare. 2021. Contrastive Behavioral Similarity Embeddings for Generalization in Reinforcement Learning. In *International Conference on Learning Representations*.
- [3] Alexander A Alemi, Ian Fischer, Joshua V Dillon, and Kevin Murphy. 2017. Deep Variational Information Bottleneck. In *International Conference on Learning Representations*.
- [4] Pablo Samuel Castro. 2020. Scalable Methods for Computing State Similarity in Deterministic Markov Decision Processes. In *AAAI Conference on Artificial Intelligence*.
- [5] Ting Chen, Simon Kornblith, Mohammad Norouzi, and Geoffrey Hinton. 2020. A Simple Framework for Contrastive Learning of Visual Representations. In *International Conference on Machine Learning*. 1597–1607.

465 [6] Norm Ferns, Prakash Panangaden, and Doina Precup. 2004. Metrics for Finite
466 Markov Decision Processes. *Proceedings of the 20th Conference on Uncertainty in
467 Artificial Intelligence* (2004), 162–169.

468 [7] Carles Gelada, Saurabh Kumar, Jacob Buckman, Ofir Nachum, and Marc G Bellemare. 2019. DeepMDP: Learning Continuous Latent Space Models for Representation Learning. In *International Conference on Machine Learning*. 2170–2179.

469 [8] Jean-Bastien Grill, Florian Strub, Florent Altché, Corentin Tallec, Pierre H
470 Richemond, Elena Buchatskaya, Carl Doersch, Bernardo Avila Pinto, Zhan Han
471 Zheng, Mohammad Azabou, et al. 2020. Bootstrap Your Own Latent: A New Approach to Self-Supervised Learning. In *Advances in Neural Information Processing Systems*.

472 [9] Danijar Hafner, Timothy Lillicrap, Jimmy Ba, and Mohammad Norouzi. 2020. Dream to Control: Learning Behaviors by Latent Imagination. In *International Conference on Learning Representations*.

473 [10] Danijar Hafner, Jurgis Pasukonis, Jimmy Ba, and Timothy Lillicrap. 2023. Mastering Diverse Domains through World Models. In *International Conference on Machine Learning*.

474

475

476

477

478

479

480

481

482

483

484

485

486

487

488

489

490

491

492

493

494

495

496

497

498

499

500

501

502

503

504

505

506

507

508

509

510

511

512

513

514

515

516

517

518

519

520

521

522

523 [11] Lihong Li, Thomas J Walsh, and Michael L Littman. 2006. Towards a Unified Theory of State Abstraction for MDPs. In *International Symposium on Artificial Intelligence and Mathematics*.

524 [12] Ilya Loshchilov and Frank Hutter. 2019. Decoupled Weight Decay Regularization. In *International Conference on Learning Representations*.

525 [13] Naftali Tishby, Fernando C Pereira, and William Bialek. 2000. The Information Bottleneck Method. *Proceedings of the 37th Allerton Conference on Communication, Control, and Computing* (2000), 368–377.

526 [14] Aaron van den Oord, Oriol Vinyals, and Koray Kavukcuoglu. 2017. Neural Discrete Representation Learning. In *Advances in Neural Information Processing Systems*.

527 [15] Jiacong Wu et al. 2026. Visual Generation Unlocks Human-Like Reasoning through Multimodal World Models. *arXiv preprint arXiv:2601.19834* (2026).

528 [16] Amy Zhang, Rowan McAllister, Roberto Calandra, Yarin Gal, and Sergey Levine. 2021. Learning Invariant Representations for Reinforcement Learning without Reconstruction. In *International Conference on Learning Representations*.

529

530

531

532

533

534

535

536

537

538

539

540

541

542

543

544

545

546

547

548

549

550

551

552

553

554

555

556

557

558

559

560

561

562

563

564

565

566

567

568

569

570

571

572

573

574

575

576

577

578

579

580